

The human cytomegalovirus microRNA miR-UL112 acts synergistically with a cellular microRNA to escape immune elimination

Daphna Nachmani¹, Dikla Lankry¹, Dana G Wolf² & Ofer Mandelboim¹

Although approximately 200 viral microRNAs are known, only very few share similar targets with their host's microRNAs. A notable example of this is the stress-induced ligand MICB, which is targeted by several distinct viral and cellular microRNAs. Through the investigation of the microRNA-mediated immune-evasion strategies of herpesviruses, we initially identified two new cellular microRNAs that targeted MICB and were expressed differently both in healthy tissues and during melanocyte transformation. We show that coexpression of various pairs of cellular microRNAs interfered with the downregulation of MICB, whereas the viral microRNAs optimized their targeting ability to efficiently downregulate MICB. Moreover, we demonstrate that through site proximity and possibly inhibition of translation, a human cytomegalovirus (HCMV) microRNA acts synergistically with a cellular microRNA to suppress MICB expression during HCMV infection.

Natural killer (NK) cells are innate lymphocytes that serve as a first line of defense against infected and transformed cells^{1–3}. Their ability to eliminate target cells is controlled by a balance between inhibitory and activating signals generated by inhibitory and activating receptors³. One of the most prominent activating receptors is NKG2D, which recognizes stress-induced ligands upregulated on the cell surface after various stresses, such as viral infection, cell transformation, DNA damage and heat shock^{4–10}. Among the human stress-induced ligands are the major histocompatibility complex class I polypeptide-related sequences MICA and MICB and the UL16-binding proteins^{4–11}.

Stress-induced ligands have a fundamental role in the recognition and elimination of hazardous cells by the immune system, and indeed strategies such as shedding of major histocompatibility complex class I-related proteins from the cell surface, retention in the endoplasmic reticulum and microRNA targeting are used by viruses, as well as by tumors, to escape NKG2D recognition and subsequent elimination^{11–16}. Thus, it is crucial to identify possible pathways that control the expression of stress-induced ligands to allow better treatment of cancer and virus-related diseases and to broaden the basic understanding of how danger is sensed by the immune system.

MicroRNAs are short noncoding RNA molecules that bind to a target transcript (mainly in the 3' untranslated region (UTR)) and repress its translation, thus controlling protein expression^{17–22}. The effect of microRNAs on protein expression is modest^{23,24}; nevertheless, these are important gene regulators, as they are involved in almost all known cellular processes^{25–28}. The expression of MICA and MICB is regulated by several cellular microRNAs, and tumors

take advantage of this regulation by upregulating the expression of these microRNAs to promote immune evasion and the generation of metastasis²⁹.

Herpesviruses create lifelong latent infections in their hosts by using a vast arsenal of immune-evasion strategies^{30,31}. Notably, human cytomegalovirus (HCMV) expresses its own microRNA to repress the translation of MICB¹⁵. Moreover, HCMV's microRNA evolved in such a way that it binds the 3' UTR of MICB at a site overlapping that of cellular microRNAs. By doing so, HCMV not only escapes NKG2D-mediated immune detection but also probably prevents the host from mutating this particular site, as it is indispensable²⁹.

The strategy of targeting MICB by a viral microRNA is not exclusive to HCMV. Epstein-Barr virus (EBV) and Kaposi's sarcoma-associated herpesvirus (KSHV) each encode a single microRNA that downregulates MICB to escape NK cell recognition¹¹. The three viral microRNAs (derived from HCMV, EBV and KSHV) do not share sequence homology^{11,15} and therefore target MICB at different binding sites.

Several pressing questions arose after the findings reported above, and we address them here. First, what has prevented the host from mutating the EBV- and KSHV-binding sites to avoid regulation by the viral microRNAs? Second, why is there such a large group of cellular microRNAs that control the expression of MICB? Third, why is it beneficial for the three viruses to generate their own specific microRNAs and not copy or use the MICB-targeting cellular microRNAs? Furthermore, why do the viruses use partially overlapping sites to target MICB and not use sites identical to those of the cellular

¹The Lautenberg Center for General and Tumor Immunology, The BioMedical Research Institute Israel Canada of the Faculty of Medicine, The Hebrew University Hadassah Medical School, Jerusalem, Israel. ²Virology Unite, Hadassah Hospital, The Hebrew University Hadassah Medical School, Jerusalem, Israel. Correspondence should be addressed to O.M. (oferm@ekmd.huji.ac.il).

Received 15 March; accepted 7 July; published online 8 August 2010; doi:10.1038/ni.1916



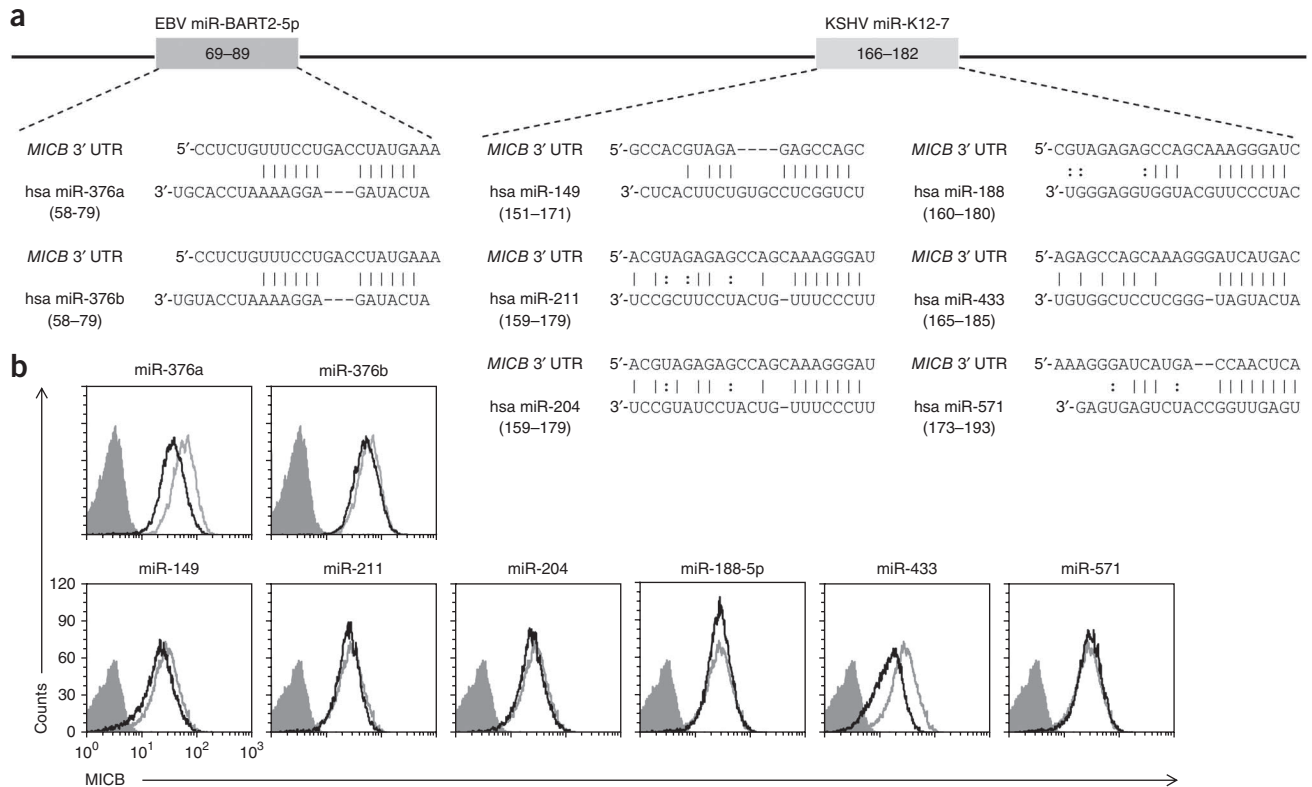


Figure 1 Newly identified cellular microRNAs that downregulate MICB. **(a)** TargetScan predictions of homo sapiens (hsa) microRNAs that bind the 3' UTR of *MICB* at binding sites overlapping those of the EBV and KSHV microRNAs. The locations of the predicted microRNAs are in parentheses. Solid lines indicate Watson-Crick base pairing; dotted lines indicate G:U wobble base pairing. **(b)** Flow cytometry analysis of MICB expression (black lines) by cells transduced with the predicted microRNAs. Gray lines, control microRNA; filled gray histograms, secondary antibody. Data are representative of six independent experiments.

microRNAs? In our view, these questions apply to almost all viral microRNAs, as many of them differ from the host's microRNAs³².

We provide here several answers to the questions above. We show that like the microRNA of HCMV, the microRNA of both EBV and KSHV bound *MICB* at sites overlapped by two cellular microRNAs. Moreover, the newly identified cellular microRNAs were expressed differently in various tissues and cell lines. In addition, whereas the cellular microRNAs interacted in an antagonizing way with each other, the viral microRNAs acted independently of the cellular microRNAs and, together with the cellular microRNAs, efficiently down-regulated *MICB*. Most notably, HCMV's microRNA miR-UL112 acted synergistically with the newly identified cellular microRNA miR-376a to repress *MICB* expression, and this interaction was dependent on site proximity and was functional during HCMV infection. Thus, we show that by creating unique microRNAs, herpesviruses generate a new, improved and, to our knowledge, never-before-reported set of viral microRNA–host microRNA interactions to escape elimination by cells of the immune system.

RESULTS

Herpesviruses exploit cellular microRNA–binding sites

As the binding sites of the EBV and KSHV microRNAs miR-BART2-5p and miR-K12-7, respectively, are located at different locations along the 3' UTR of *MICB* (Fig. 1a), we sought to determine whether, like the microRNA of HCMV²⁹, the microRNAs of EBV and KSHV also bind at sites overlapping those of cellular microRNAs. To address this issue, we initially used the online algorithm TargetScan to search for cellular microRNAs predicted to bind *MICB* at sites that overlap those

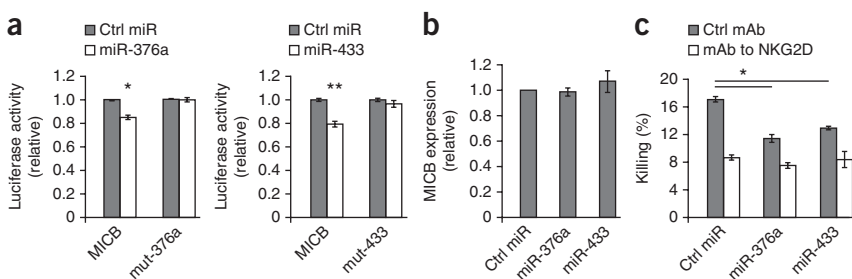
of the viral microRNAs. This scan identified two cellular microRNAs predicted to target *MICB* at a site overlapping the binding site for EBV's miR-BART2-5p, as well as several cellular microRNAs predicted to bind *MICB* at the binding site for KSHV's miR-K12-7 (Fig. 1a). To test whether the predicted microRNAs could indeed downregulate *MICB*, we cloned all of them into lentiviral constructs containing a green fluorescent protein (GFP) cassette, which allowed us to monitor transduction efficiency (Supplementary Fig. 1a), and transduced the constructs into *MICB*-expressing cells. The lentiviral transduction was extremely efficient (Supplementary Fig. 1), and we monitored *MICB* expression on GFP⁺ cells. Of all the predicted microRNAs, only miR-376a (from the EBV-overlapping group) and miR-433 (from the KSHV-overlapping group) showed substantial downregulation of *MICB* expression (Fig. 1b and Supplementary Fig. 1b). We confirmed expression of miR-376a and miR-433 in the transduced cells by quantitative real-time PCR (Supplementary Table 1).

We also tested whether miR-376a and miR-433 control *MICA* expression. Although miR-376a was predicted by TargetScan to bind the 3' UTR of *MICA*, the downregulation of *MICA* by the microRNA was not consistent. No binding sites for miR-433 in the 3' UTR of *MICA* were predicted. In addition, because all viral microRNAs derived from HCMV, EBV and KSHV target only *MICB*, we continued our analysis with *MICB*.

MiR-376a and miR-433 diminish NK cell–mediated cytotoxicity

A single microRNA is estimated to target approximately 300 genes^{19,33}. To demonstrate that miR-376a and miR-433 directly bound to *MICB* at the predicted binding sites (Fig. 1a), we did a dual

Figure 2 The microRNAs miR-376a and miR-433 directly bind the 3' UTR of *MICB*, repress its translation and reduce NK cell cytotoxicity. **(a)** Luciferase activity in DU145 cells transduced with control microRNA (Ctrl miR), miR-376a (left) or miR-433 (right) and transfected with reporter plasmids (horizontal axis); results are presented relative to control reporter activity. *MICB*, reporter containing the wild-type 3' UTR of *MICB*; mut-376a and mut-433, reporters mutated at seed sequence of the miR-376a- and miR-433-binding sites, respectively. * $P < 0.01$ and ** $P < 0.03$ (two-tailed Student's *t*-test). Data are representative of three independent experiments (mean \pm s.e.m. of triplicates). **(b)** Quantitative real-time PCR analysis of *MICB* mRNA in RKO cells transduced with control microRNA, miR-376a or miR-433, presented relative to mRNA for the human ribosomal protein L32. Data are representative of three independent experiments (average mean \pm s.e.m.). **(c)** Killing of labeled RKO cells, expressing control microRNA, miR-376a or miR-433, by bulk primary NK cells preincubated with isotype-matched control monoclonal antibody (Ctrl mAb) or monoclonal antibody to NKG2D mAb (mAb to NKG2D), assessed after 5 h of coinubation. * $P < 0.02$ (two-tailed Student's *t*-test). Data are representative of three independent experiments with NK cells from different donors (mean \pm s.e.m. of triplicates).



luciferase reporter assay. For this we generated three firefly luciferase constructs: one contained the wild-type 3' UTR of *MICB*; one was mutated at the 3' UTR of *MICB* at the 'seed sequence' of the predicted miR-376a-binding site; and another was mutated at the seed sequence of the predicted miR-433-binding site. We transiently transfected these constructs into DU145 human prostate cancer cells that had been transduced with miR-376a, miR-433 or a control microRNA. Luciferase activity was repressed in cells expressing the microRNAs (Fig. 2a), and mutations at the seed sequences of the predicted sites completely abolished the repression mediated by each microRNA (Fig. 2a). This indicated that the predicted binding sites were indeed targeted by the microRNAs identified. Next, to elucidate the mechanism of this repression, we did quantitative real-time PCR analysis of RKO cells transduced with either miR-376a or miR-433 and evaluated the abundance of the *MICB* transcript. We did not find any significant difference between cells expressing the microRNAs and control cells

in the abundance of *MICB* transcripts (Fig. 2b), which suggested that the microRNAs' mode of action was translational repression and not mRNA degradation. Finally, we found that the lower expression of *MICB* mediated by miR-376a and miR-433 was functional, as it led to less recognition and killing of the transduced cells by NK cells (Fig. 2c). This effect was NKG2D specific, as an NKG2D-blocking antibody decreased the killing of all transduced cells to equivalent amounts (Fig. 2c).

Expression pattern of the *MICB*-targeting microRNAs

We demonstrated above that miR-376a and miR-433 downregulated *MICB*, thus adding them to a relatively large group of previously identified *MICB*-targeting cellular microRNAs²⁹ (Fig. 3). We next sought to determine why humans would need nine different microRNAs (the seven identified before (miR-17, miR-20, miR-93, miR-106, miR-372, miR-373 and miR-520)²⁹ and the two identified here (miR-376a and

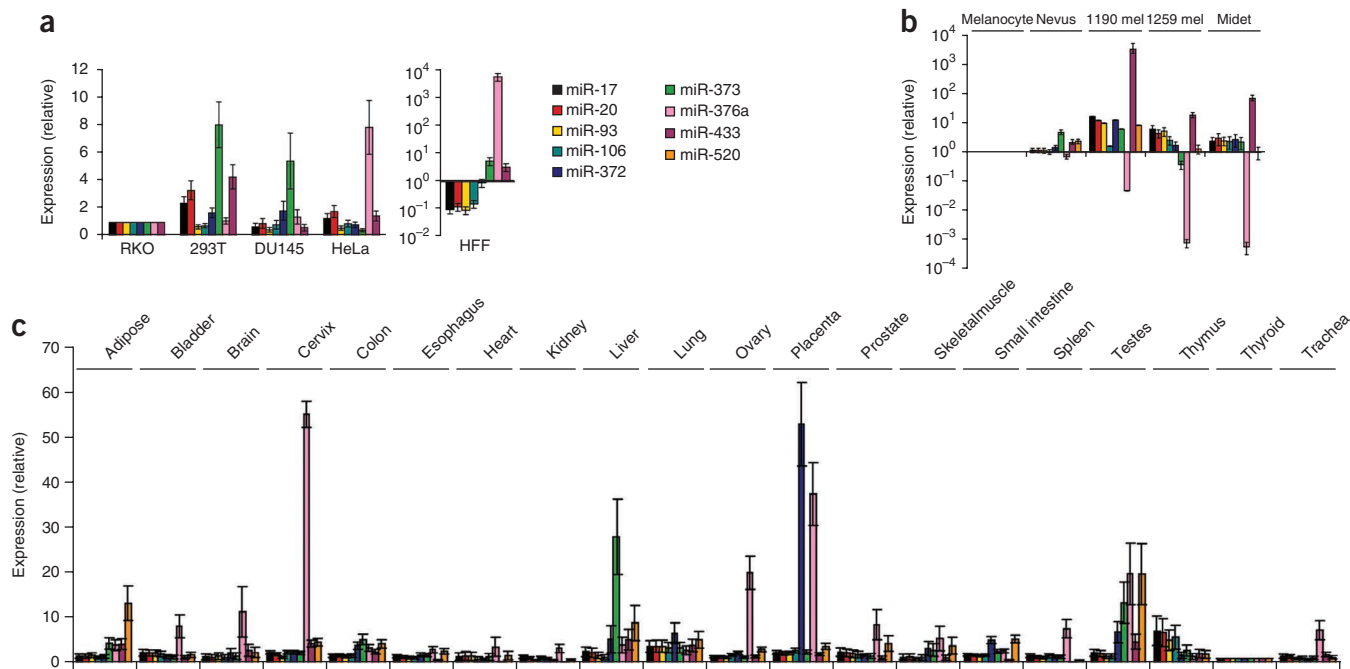


Figure 3 Expression patterns of *MICB*-targeting microRNAs in various cell lines and in healthy human tissues. **(a–c)** Quantitative real-time PCR analysis of *MICB*-targeting cellular microRNAs (key) in human cell lines (**a**, left) and HFF cells (**a**, right), at various stages of melanocyte transformation in metastatic melanoma cell lines (1190 mel, 1259 mel and Midet; **b**), and in healthy human tissues (**c**), presented relative to the abundance of U6 small RNA in RKO cells (**a**), melanocytes (**b**) or thyroid tissue (**c**). Data are from three independent experiments (average mean \pm s.e.m.).

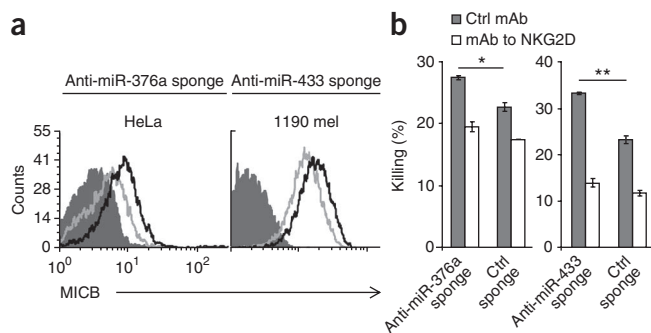


Figure 4 MICB expression is upregulated in cell lines expressing anti-microRNA sponges, which results in increased killing by NK cells. **(a)** Flow cytometry of MICB expression by HeLa cells (left) transduced with an anti-miR-376a sponge (black line) or a control sponge (gray line) or by 1190 mel cells (right) transduced with an anti-miR-433 sponge (black line) or a control sponge (gray line). Filled gray histograms, secondary antibody staining. Data are representative of three independent experiments. **(b)** Killing of labeled HeLa cells (expressing an anti-miR-376a sponge or a control sponge (Ctrl sponge); left) or labeled 1190 mel cells (expressing an anti-miR-433 sponge or a control sponge; right) by bulk NK cells preincubated with isotype-matched control monoclonal antibody or monoclonal antibody to NKG2D, assessed after 5 h of coinoculation. * $P = 0.009$ and ** $P = 0.012$ (two-tailed Student's t -test). Data are representative of three independent experiments with NK cells derived from different donors (mean \pm s.e.m. of triplicates).

miR-433)) to control MICB expression. We hypothesized that one reason for this might be differences in the expression patterns of the various microRNAs in different tissues and, consequently, in cell lines. Indeed, as we predicted, we observed different patterns of expression of the various MICB-targeting microRNAs in several cell lines (293T human embryonic kidney cells, RKO human colon carcinoma cells, HeLa human cervical cancer cells and DU145 cells) and in primary human foreskin fibroblast (HFF) cells (Fig. 3a). We found that miR-520 was the only microRNA not expressed by the cell lines tested (Fig. 3a). We also tested expression of the MICB-targeting microRNAs during melanoma tumor development (Fig. 3b). Notably, we observed an increase in the expression of some of the microRNAs along such development, beginning with normal melanocytes, then proceeding through nevus stage and ending in metastatic melanoma (Fig. 3b). The two microRNAs with the greatest change in expression during melanoma development were miR-376a, which was downregulated by melanoma cells and miR-433, which was upregulated, (Fig. 3b).

It is established that MICB protein is absent in healthy tissues, whereas MICB mRNA is expressed in many if not all healthy tissues^{34,35} (Supplementary Fig. 2). Because of this discrepancy, it was critical that we confirm that the microRNAs were expressed together with their target gene, *MICB*. Indeed, all of the microRNAs identified as targeting *MICB* were expressed in all the tissues we examined (Fig. 3c). Some microRNAs showed differences in expression across the various tissues. In particular, miR-376a had higher expression in bladder, brain, cervix, ovary, placenta, prostate, skeletal muscle, spleen, testis and trachea than in other tissues (Fig. 3c).

Endogenous control of MICB expression

Our next goal was to demonstrate that miR-376a and miR-433 endogenously control MICB expression. For this purpose we generated two 'sponge' constructs directed against miR-376a and miR-433, as well as a control sponge. These constructs contain multiple binding sites for the desired microRNA and are located downstream of a GFP cassette.

Thus, these sponges function as decoy transcripts and sequester the specific microRNA from its original target^{11,36}.

We transduced two tumor cell lines with relatively high expression of the relevant microRNAs, HeLa and the melanoma cell line 1190 mel (Fig. 3a,b), with the anti-microRNA sponges anti-miR-376a and anti-miR-433, respectively, and monitored transduction efficiency by GFP expression (Supplementary Fig. 3a). As predicted, the presence of the anti-microRNA sponges resulted in a higher expression of MICB in GFP⁺ cells of both cell lines (Fig. 4a and Supplementary Fig. 3b). This upregulation resulted in increased NK cell recognition and NKG2D-dependent elimination of the transduced cells (Fig. 4b). These combined results suggest that the EBV- and KSHV-encoded microRNAs do not target random sites in MICB. These viruses possibly use a strategy in which they target a microRNA-binding site already in use by cellular microRNAs, thus making it extremely difficult for the host to escape viral regulation by mutating the relevant binding site.

Human and viral microRNA cooperation

The relatively large number of cellular microRNAs that target MICB (nine in total²⁹; Fig. 5a), together with the observation that all of them were expressed (albeit in different amounts; Fig. 3c) in all tissues tested, raised the following question: why are so many different cellular microRNAs needed to control MICB expression? Perhaps these various cellular microRNAs act together to downregulate MICB more efficiently? To test that hypothesis, we transduced RKO cells with a single cellular microRNA or with a pair of cellular microRNAs and analyzed MICB expression by flow cytometry (Fig. 5b and Supplementary Fig. 4). The transduction efficiency of all combinations was nearly 100% (Supplementary Fig. 4a), quantitative real-time PCR analysis confirmed the expression of the microRNAs in all of the combinations (Supplementary Table 1), and we gated on the GFP⁺ cells for flow cytometry analysis. From the group of

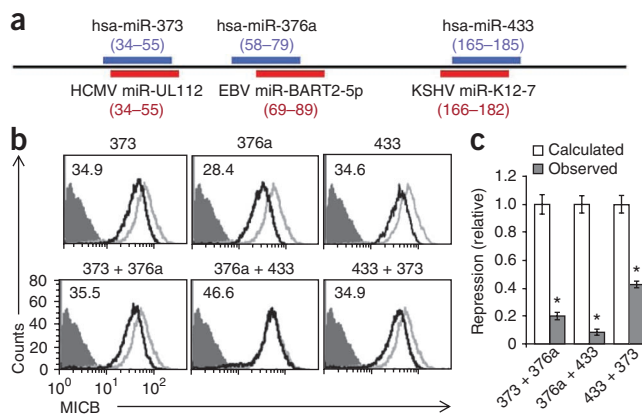
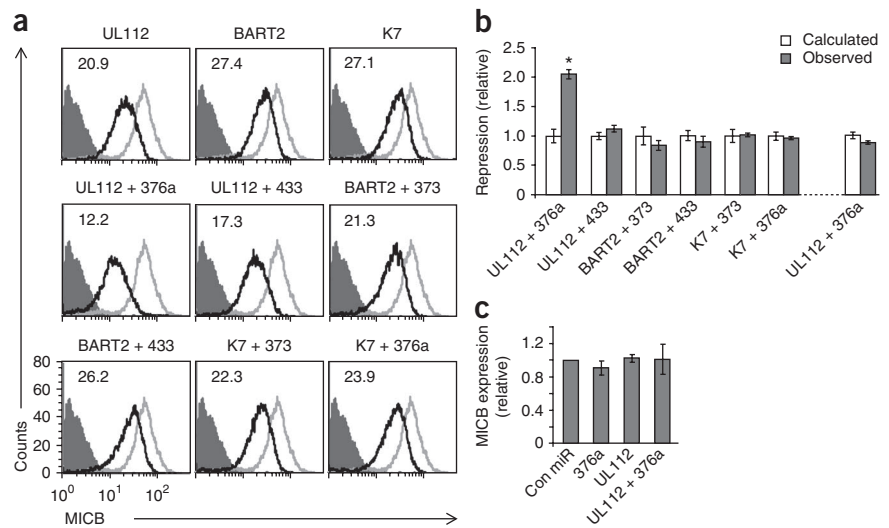


Figure 5 Coexpression of cellular microRNAs antagonizes the repression of MICB expression. **(a)** Binding sites (lines) and locations (numbers in parentheses) of cellular microRNAs (blue) and viral microRNAs (red) along the 3' UTR of *MICB*. **(b)** Flow cytometry of MICB expression (black lines) by RKO cells transduced with a single microRNA (top row) or a pair of cellular microRNAs (bottom row): 373, miR-373; 376a, miR-376a; 433, miR-433. Gray lines, control microRNA; filled gray histograms, secondary antibody. Numbers in top left corners indicate mean fluorescent intensity of MICB expression. Data are representative of four independent experiments. **(c)** Luciferase repression in RKO cells transduced with paired or single microRNAs and transfected with the *MICB* 3' UTR reporter plasmid, presented as described in Results. * $P < 0.0001$ (two-tailed Student's t -test). Data are representative of three independent experiments (mean \pm s.e.m. of triplicates).

Figure 6 The microRNAs miR-UL112 and miR-376a act synergistically to downregulate MICB expression. **(a)** Flow cytometry of MICB expression (black lines) by RKO cells transduced with a single viral microRNA (top row) or with a pair of one viral and one cellular microRNA (middle and bottom rows): UL112, miR-UL112 (HCMV); BART2, miR-BART2-5p (EBV); K7, miR-K12-7 (KSHV). Gray lines, control microRNA; gray filled histograms, secondary antibody. Numbers in top left corners indicate mean fluorescent intensity of MICB expression. Data are representative of three independent experiments. **(b)** Luciferase repression in RKO cells transduced with microRNA pairs as described in **a** and transfected with the *MICB* 3' UTR reporter plasmid (left) or a reporter containing the 3' UTR of *MICB* in which the site for miR-UL112 was relocated (far right), presented as described in Results. * $P < 0.006$ (two-tailed Student's *t*-test).



Data are representative of three independent experiments (mean \pm s.e.m. of triplicates). **(c)** Quantitative real-time PCR analysis of *MICB* mRNA in RKO cells transduced with a control microRNA, miR-376a or miR-UL112, or both together, presented relative to mRNA for the human ribosomal protein L32. Data are from three independent experiments (average mean \pm s.e.m.).

cellular microRNAs that target *MICB* at a site overlapping that of HCMV's miR-UL112, we selected a single representative microRNA, miR-373 (ref. 29; Fig. 5a). As noted before²⁹ and reported here, *MICB* was downregulated by all of the cellular microRNAs when they were expressed singly (Fig. 5b and Supplementary Fig. 4b). Unexpectedly, when the various pairs of cellular microRNAs were coexpressed, the downregulation of *MICB* seemed to be impaired (Fig. 5b and Supplementary Fig. 4b), and coexpression of miR-376a and miR-433 almost completely abolished the downregulation of *MICB* (Fig. 5b and Supplementary Fig. 4b).

We used a dual luciferase reporter assay to quantify the interactions reported above and to demonstrate that coexpression of the various cellular microRNAs indeed resulted in an antagonizing effect. We measured the extent of cooperation by calculating firefly luciferase repression relative to that of renilla luciferase. The 'calculated' repression by the microRNAs was the linear summation of the repression by each single microRNA, and the 'observed' repression was the actual repression observed when the microRNAs were coexpressed (Fig. 5c). In agreement with the flow cytometry data (Fig. 5b and Supplementary Fig. 4), for each pair of microRNAs the observed repression was much lower than the calculated repression and the greatest antagonistic effect occurred when miR-376a and miR-433 were coexpressed (Fig. 5c). Notably, the change in expression of miR-376a and miR-433 during melanoma progression was reciprocal (Fig. 3b), perhaps to avoid such an antagonistic effect.

Like the cellular microRNAs, it seemed that the viral microRNAs interfered with each other in the downregulation of *MICB* when coexpressed (Supplementary Fig. 5). However, the relevance of such interactions is questionable because coinfection of the same cell *in vivo* with these viruses is rare. Thus, we next turned to study what are probably the most critical interactions, those between the viral microRNAs and the cellular microRNAs. For this we transduced RKO cells with a single viral microRNA or with pairs of viral and cellular microRNAs (Fig. 6a and Supplementary Fig. 6a). The transduction efficiency of all combinations was nearly 100% (Supplementary Fig. 6). Quantitative real-time PCR analysis confirmed expression of the microRNAs in all of the combinations (Supplementary Table 1), and we gated on GFP⁺ cells for flow cytometry analysis. We chose pairs

of cellular and viral microRNAs that do not target an overlapping site, because as expected, overlapping pairs showed competitive interaction with each other (data not shown).

Unexpectedly, analysis of the various microRNA pairs did not indicate any antagonizing interactions between the viral and cellular microRNAs (Fig. 6a and Supplementary Fig. 6b). In contrast, it seemed as if coexpression of the viral and cellular microRNAs acted independently of each other, which resulted in an additive effect on the downregulation of *MICB* (Fig. 6b). One exception was the duo of HCMV's miR-UL112 and cellular miR-376a. When these microRNAs were coexpressed, they acted synergistically in downregulating *MICB* expression (twofold greater than the predicted additive value; Fig. 6b).

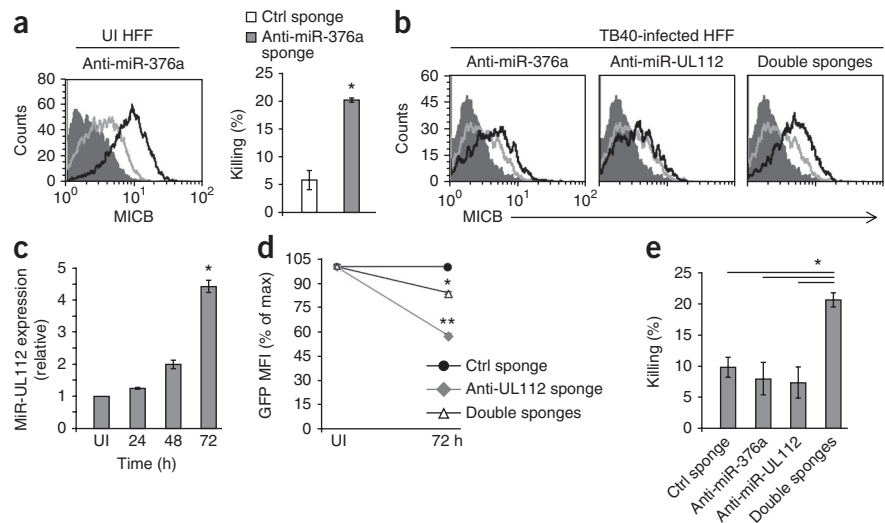
Synergistic mechanisms

It has been demonstrated with artificial microRNA-binding sites that site proximity (a distance up to ~50 nucleotides) might be a crucial factor in determining cellular microRNA cooperation^{37,38}. As miR-UL112 and miR-376a are 24 nucleotides apart (from the 5' end of miR-UL112 to the 5' end of miR-376a; Supplementary Table 2), we sought to determine whether site proximity might be a critical determinant in the synergism observed between these particular cellular and viral microRNAs. For this we mutated the binding site of miR-UL112 in the 3' UTR of *MICB* and then relocated it ~850 nucleotides downstream of its original location. We transiently transfected the firefly constructs into RKO cells transduced with miR-UL112 or miR-376a alone, the two together, or a control microRNA. The relocated site of miR-UL112 was still functional, as it repressed firefly luciferase activity to the same extent as the wild-type binding site did (Supplementary Fig. 7). Notably, despite the observation that luciferase repression was similar with the binding site in either location, relocation of the miR-UL112-binding site abolished the synergistic interaction between miR-UL112 and miR-376a, whereas an additive effect still remained (Fig. 6b, far right, and Supplementary Fig. 7).

Figure 7 Synergistic control of MICB expression by miR-376a and miR-UL112 during HCMV infection. (a) Flow cytometry of MICB expression (left) by uninfected (UI) HFF cells transduced with an anti-miR-376a sponge (black line) or a control sponge (gray line), and killing of those HFF cells (right) by bulk NK cells. Gray filled histogram (left), secondary antibody. * $P = 0.004$ (two-tailed Student's t -test).

Data are representative of three independent experiments (right, mean \pm s.e.m. of triplicates, with NK cells derived from different donors). (b) MICB expression (black lines) by HFF cells transduced with the anti-miR-376a sponge or anti-miR-UL112 sponge or both together (Double sponges) and infected for 72 h with the TB40 strain of HCMV. Gray lines, control sponge; gray filled histograms, secondary antibody. Data are representative of three independent experiments. (c) Quantitative RT-PCR analysis of miR-UL112 in HFF cells infected for 24, 48 or 72 h with the TB40 strain of HCMV, presented relative to U6 small RNA in uninfected HFF cells. * $P < 6 \times 10^{-5}$, compared with uninfected (two-tailed Student's t -test). Data are from three independent experiments (average mean \pm s.e.m.).

(d) GFP expression in HFF cells transduced with a control sponge, an anti-miR-UL112 sponge or with both anti-miR-UL112 and anti-miR-376a sponges, assessed 72 h after infection with the TB40 strain of HCMV. * $P = 5.6 \times 10^{-10}$ and ** $P = 3.4 \times 10^{-12}$, compared with control sponge (two-tailed Student's t -test). Data are representative of three independent experiments (mean \pm s.e.m. of six replicates). (e) Killing of labeled HFF cells (infected as described in c) by bulk NK cells. * $P < 0.001$ (two-tailed Student's t -test). Data are representative of three independent experiments with NK cells derived from different donors (mean \pm s.e.m. of triplicates).



To test whether translation inhibition or mRNA degradation was the mechanism responsible for the observed synergistic effect, we did quantitative real-time PCR analysis of the abundance of the MICB transcript in RKO cells transduced with either a single microRNA or coexpressing the microRNAs. We observed no change in MICB transcript abundance (Fig. 6c). Thus, site proximity is indeed a critical determinant in the synergistic downregulation of MICB by miR-376a and miR-UL112, which probably occurs by inhibition of translation.

Synergism during HCMV infection

Our final goal was to demonstrate synergistic cooperation of miR-376a and miR-UL112 during HCMV infection. As HFF cells could be infected by HCMV and had relatively high expression of miR-376a (Fig. 3a), we initially sought to determine whether miR-376a endogenously controls MICB expression in HFF cells, as it did in HeLa cells (Fig. 4a). For this, we transduced HFF cells with the anti-miR-376a sponge and a control sponge. We obtained nearly 100% efficiency of transduction (Supplementary Fig. 8a) and analyzed the expression of MICB on GFP⁺ cells by flow cytometry (Fig. 7a). Indeed, HFF cells expressing the anti-miR-376a sponge had much higher MICB expression (Fig. 7a and Supplementary Fig. 8b), which indicated that miR-376a endogenously controlled MICB expression in these primary cells. Moreover, the higher MICB expression influenced NK cell recognition, as we observed increased killing of cells transduced with anti-miR-376a by NK cells (Fig. 7a, right).

Next we investigated the role of miR-376a and of miR-UL112 during HCMV infection. For this we transduced HFF cells with the anti-miR-376a sponge or anti-miR-UL112 sponge, both sponges together, or a control sponge. The transduction efficiency was, as usual, close to 100% (Supplementary Fig. 8a), and we verified expression of the various sponges by PCR (data not shown). Next we infected all cells with the TB40 strain of HCMV. MICB expression remained low in the infected cells transduced with the control sponge during the entire experiment, as both viral and cellular

mechanisms operate to downregulate the expression of MICB^{15,31} (Fig. 7b and Supplementary Fig. 8c, gray line).

At 48 h after infection, the presence of the cellular or viral sponges resulted in higher MICB expression, and when both sponges were coexpressed there was only a small additional increase in MICB expression (Supplementary Fig. 8c,d). However, 72 h after infection, the effect of the sponges was altered. The presence of either the anti-miR-376a sponge or the anti-miR-UL112 sponge resulted in minimally higher MICB expression (Fig. 7b and Supplementary Fig. 8e). Yet—and most importantly—at 72 h after infection, when both cellular and viral sponges were coexpressed, the increase in MICB expression was greater than it was with either of the sponges alone (Fig. 7b right and Supplementary Fig. 8e).

The changes reported above in the effect of the sponges along the course of infection were probably due to the accumulation of miR-UL112 as infection was prolonged³⁹ (Fig. 7c). Thus, the anti-miR-376a sponge was less effective after 72 h of infection than after 48 h, probably because miR-UL112 was present in large amounts and diminished MICB expression. These large quantities of miR-UL112 at 72 h after infection probably could not be completely 'titrated out' by the anti-miR-UL112 sponge. Indeed, the GFP expression of the anti-miR-UL112 sponge decreased as infection progressed, probably because of sponge destruction mediated by the increasing amounts of miR-UL112 (Fig. 7d). We found over 40% less GFP in cells transduced with the anti-miR-UL112 sponge, whereas we found around 15% less in infected cells expressing both sponges (Fig. 7d). The presence of the anti-miR-376a sponge in cells transduced with both sponges together probably explained the difference in GFP loss (40% versus 15%), as its GFP expression did not change during the infection.

Finally, to test the physiological implications of the synergism described above, we tested the ability of NK cells to eliminate the transduced and infected cells. In complete agreement with the flow cytometry data (Fig. 7b and Supplementary Fig. 8), only the infected HFF cells transduced with both sponges showed increased elimination by NK cells (Fig. 7e and Supplementary

Fig. 8), which demonstrates the importance of the synergistic mechanism of miR-UL112 and miR-376a during HCMV infection.

DISCUSSION

Through the investigation of two herpesvirus microRNAs of EBV and KSHV, we initially identified two cellular microRNAs, miR-376a and miR-433, that regulated expression of the stress-induced ligand MICB. These two cellular microRNAs bound the 3' UTR of *MICB* at sites overlapping the EBV microRNA- and KSHV microRNA-binding sites, respectively. By targeting an overlapping site, the viruses probably prevent the host from inserting mutations in *MICB* to avoid viral targeting.

The effect of microRNAs in general is modest^{23,24}. However, we have shown here that such a modest effect was sufficient to control *MICB* expression under normal conditions and that when we neutralized the microRNA effect endogenously, *MICB* appeared on the cell surface. Our observations and the identification of nine *MICB*-targeting microRNAs and seven *MICA*-targeting microRNAs (as reported here and in ref. 29) might explain published observations in the field demonstrating the existence of both *MICA* mRNA and *MICB* mRNA in many healthy tissues and the absence of *MICA* and *MICB* proteins⁴. We have demonstrated that the microRNAs were present in all tissues examined and we therefore suggest that these microRNAs 'titrate' *MICB* expression and also *MICA* expression under normal conditions to avoid autoimmunity. Alterations in microRNA amounts^{40,41} or changes in the amount of *MICA* mRNA and *MICB* mRNA after infection²⁹ would therefore result in the expression of *MICA* and *MICB* and the elimination of the hazardous cell by cells of the immune system.

The identification of the two cellular microRNAs presented here (miR-376a and miR-433) opened the door for the investigation of another issue: viral and cellular microRNA cooperation. As so many microRNAs control *MICB* expression, it was critical for us to explore the nature of the interactions between them. This investigation was made possible because miR-376a and miR-433 bind *MICB* at sites distinct from that of all other previously identified *MICB*-targeting microRNAs.

Unexpectedly, when the cellular *MICB*-targeting microRNAs were coexpressed (especially miR-376a and miR-433), they antagonized each other's effect. This observation might explain the reciprocal expression patterns of miR-376a and miR-433 observed in various melanomas and some healthy tissues. The advantage of the antagonizing interactions between the cellular microRNAs is probably the fine tuning they provide to the cellular control of *MICB* expression.

The sequences of the cellular and viral microRNAs examined are different, especially at the seed region^{11,15,29}. Thus, all three viral microRNAs bind the 3' UTR of *MICB* at distinct sites, yet these sites overlapped the binding sites of the cellular microRNAs. This prompted us to ask why it would be more beneficial for all three herpesviruses to create a new *MICB*-targeting viral microRNA rather than copying an existing microRNA or manipulating the regulation of the cellular microRNAs. Such strategies are already in use by few viral microRNAs; the KSHV-encoded miR-K12-11 has a seed sequence similar to that of the cellular microRNA miR-155, which has an important role in B cell development and tumor transformation^{42,43}. Thus, as these microRNAs target a common pool of transcripts, KSHV is able to influence B cell differentiation and probably also tumor transformation. Additionally, EBV-infected cells have large amounts of miR-155. This upregulation is mediated mainly by the viral protein LMP-1, which modulates the expression of *BIC*, the miR-155 precursor⁴⁴. So what would prevent the viral microRNAs explored here (or any other viral microRNA, for that

matter) from using a similar strategy? The hypothesis that the relevant cellular microRNAs are downregulated when cells are infected with the various viruses is probably incorrect, as HCMV infection does not alter the expression of *MICB*-targeting cellular microRNAs²⁹. Another possibility is that the viral microRNAs differ from the host's microRNAs, so they could affect both viral and cellular genes. For example, HCMV's miR-UL112 targets the cellular gene *MICB*²⁹ and the viral genes *IE72* and *UL114* (refs. 29,45,46). However, it is unlikely that all viral microRNAs target both cellular and viral genes and that viral microRNAs have unique sequences because of that.

Thus, perhaps the most likely option is that by generating their own microRNAs, the viruses optimize their ability to target cellular genes either individually or as a unified force together with cellular microRNAs. Indeed, we have shown here that in contrast to the cellular microRNAs, the pairs of viral and cellular microRNAs did not interfere with each other's effect; in contrast, their downregulation of *MICB* was independent of one another, which resulted in an additive effect. Notably, despite the difficulties of investigating this synergistic phenomenon during HCMV infection (because of various mechanisms present during infection), we observed that miR-UL112 and miR-376a indeed acted synergistically during HCMV infection to control *MICB* expression.

The physiological relevance of the viral and cellular synergism could not be addressed *in vivo* in an animal model. HCMV is completely different from mouse CMV and cannot infect mice. Furthermore, mouse CMV viral microRNAs are totally different from the human CMV ones, and there are no mouse viral microRNAs identified yet that downregulate the stress-induced ligands of the mouse. Most notably, *MICB* (the subject of this paper) is not expressed in mice. The *MICB*-viral microRNA relationship is an example of how human viruses that coevolved with their natural human host develop unique mechanisms specific only to the human viruses and to the human host to escape recognition and elimination by cells of the immune system.

We have demonstrated the physiological relevance of the synergistic effect of the HCMV viral microRNA miR-UL112 and the cellular microRNA miR-376a with killing experiments and sponges directed against both microRNAs during authentic HCMV infection. We have shown that the synergistic mechanism of miR-UL112 and miR-376a probably involves inhibition of protein translation and that it is also dependent on the proximity of the microRNA-binding sites. Although site proximity was a necessity, it was not sufficient for the creation of the synergistic interaction observed. The 24 nucleotides that separate miR-UL112 and miR-376a also separate the cellular microRNAs miR-373 and miR-376a, yet these cellular microRNAs do not act together but instead interfere with each other's effect. From this we can conclude that additional factors are also involved in the interactions between microRNAs; such factors might be intrinsic to the sequence of the microRNA or to the target mRNA. In this context, miR-UL112 is indeed a unique microRNA in this group of *MICB*-targeting microRNAs. Whereas all the cellular microRNAs and the EBV and KSHV microRNAs have a full 'seed' match and bulges in their 3' pairing, miR-UL112 has two mismatches in its seed region and full binding of its the 3' end to the UTR of *MICB*¹⁵. In summary, we have provided new insight into virus-host interactions and suggest that viruses developed their own microRNAs to more efficiently target the host's genes. The cooperative regulation demonstrated here brings a new dimension into viral manipulations, as together with the host microRNAs, viruses (through their unique microRNA repertoire) can act in synergy with, antagonize or be inert in the regulation of cellular genes.

METHODS

Methods and any associated references are available in the online version of the paper at <http://www.nature.com/natureimmunology/>.

Note: Supplementary information is available on the Nature Immunology website.

ACKNOWLEDGMENTS

We thank A. Bernard (Hôpital de l'Archet, Nice, France) for monoclonal anti-CD99 (12E7); Y. Livneh, D. Davis and S. Jonjic and all members of the Mandelboim laboratory for suggestions and discussions and for critical reading of the manuscript; S. Diederichs and W. Filipowicz for discussions and suggestions; and M. Lotem and team (Hadassah Hospital) for primary melanocytes and nevi. Supported by The Israeli Science Foundation (O.M.), The Israeli Science Foundation (Morasha, to O.M.), Croatia-Israel Research (O.M.), Ministry of Science and Technology-Deutsches Krebsforschungszentrum (O.M.), The European Consortium (MRTN-CT-2005 to O.M.), Rosetrees Trust (O.M.), the Israel Cancer Association (20100003 to O.M.) and the Association for International Cancer Research (O.M.).

AUTHOR CONTRIBUTIONS

D.N. did all experiments, analyzed the data and wrote the paper; D.L. and D.G.W. provided reagents; and O.M. supervised the project.

COMPETING FINANCIAL INTERESTS

The authors declare no competing financial interests.

Published online at <http://www.nature.com/natureimmunology/>.

Reprints and permissions information is available online at <http://npg.nature.com/reprintsandpermissions/>.

- Guerra, N. *et al.* NKG2D-deficient mice are defective in tumor surveillance in models of spontaneous malignancy. *Immunity* **28**, 571–580 (2008).
- Lakshmikanth, T. *et al.* NCRs and DNAM-1 mediate NK cell recognition and lysis of human and mouse melanoma cell lines in vitro and in vivo. *J. Clin. Invest.* **119**, 1251–1263 (2009).
- Arnon, T.I., Markel, G. & Mandelboim, O. Tumor and viral recognition by natural killer cells receptors. *Semin. Cancer Biol.* **16**, 348–358 (2006).
- Eagle, R.A. & Trowsdale, J. Promiscuity and the single receptor: NKG2D. *Nat. Rev. Immunol.* **7**, 737–744 (2007).
- Gasser, S., Orsulic, S., Brown, E.J. & Raulet, D.H. The DNA damage pathway regulates innate immune system ligands of the NKG2D receptor. *Nature* **436**, 1186–1190 (2005).
- Gasser, S. & Raulet, D.H. Activation and self-tolerance of natural killer cells. *Immunol. Rev.* **214**, 130–142 (2006).
- Gonzalez, S., Groh, V. & Spies, T. Immunobiology of human NKG2D and its ligands. *Curr. Top. Microbiol. Immunol.* **298**, 121–138 (2006).
- Groh, V. *et al.* Cell stress-regulated human major histocompatibility complex class I gene expressed in gastrointestinal epithelium. *Proc. Natl. Acad. Sci. USA* **93**, 12445–12450 (1996).
- Groh, V., Steinle, A., Bauer, S. & Spies, T. Recognition of stress-induced MHC molecules by intestinal epithelial gammadelta T cells. *Science* **279**, 1737–1740 (1998).
- Venkataraman, G.M., Suci, D., Groh, V., Boss, J.M. & Spies, T. Promoter region architecture and transcriptional regulation of the genes for the MHC class I-related chain A and B ligands of NKG2D. *J. Immunol.* **178**, 961–969 (2007).
- Nachmani, D., Stern-Ginossar, N., Sarid, R. & Mandelboim, O. Diverse herpesvirus microRNAs target the stress-induced immune ligand MICB to escape recognition by natural killer cells. *Cell Host Microbe* **5**, 376–385 (2009).
- Dobrovina, E.S. *et al.* Evasion from NK cell immunity by MHC class I chain-related molecules expressing colon adenocarcinoma. *J. Immunol.* **171**, 6891–6899 (2003).
- Dranoff, G. Targets of protective tumor immunity. *Ann. NY Acad. Sci.* **1174**, 74–80 (2009).
- Groh, V., Wu, J., Yee, C. & Spies, T. Tumor-derived soluble MIC ligands impair expression of NKG2D and T-cell activation. *Nature* **419**, 734–738 (2002).
- Stern-Ginossar, N. *et al.* Host immune system gene targeting by a viral miRNA. *Science* **317**, 376–381 (2007).
- Wilkinson, G.W. *et al.* Modulation of natural killer cells by human cytomegalovirus. *J. Clin. Virol.* **41**, 206–212 (2008).
- Ambros, V. The functions of animal microRNAs. *Nature* **431**, 350–355 (2004).
- Bartel, D.P. MicroRNAs: genomics, biogenesis, mechanism, and function. *Cell* **116**, 281–297 (2004).
- Bartel, D.P. MicroRNAs: target recognition and regulatory functions. *Cell* **136**, 215–233 (2009).
- Chekulaeva, M. & Filipowicz, W. Mechanisms of miRNA-mediated post-transcriptional regulation in animal cells. *Curr. Opin. Cell Biol.* **21**, 452–460 (2009).
- Du, T. & Zamore, P.D. microPrimer: the biogenesis and function of microRNA. *Development* **132**, 4645–4652 (2005).
- Du, T. & Zamore, P.D. Beginning to understand microRNA function. *Cell Res.* **17**, 661–663 (2007).
- Baek, D. *et al.* The impact of microRNAs on protein output. *Nature* **455**, 64–71 (2008).
- Selbach, M. *et al.* Widespread changes in protein synthesis induced by microRNAs. *Nature* **455**, 58–63 (2008).
- Carrington, J.C. & Ambros, V. Role of microRNAs in plant and animal development. *Science* **301**, 336–338 (2003).
- Davidson-Moncada, J., Papavasiliou, F.N. & Tam, W. MicroRNAs of the immune system: roles in inflammation and cancer. *Ann. NY Acad. Sci.* **1183**, 183–194 (2010).
- Garzon, R., Calin, G.A. & Croce, C.M. MicroRNAs in cancer. *Annu. Rev. Med.* **60**, 167–179 (2009).
- Yekta, S., Tabin, C.J. & Bartel, D.P. MicroRNAs in the Hox network: an apparent link to posterior prevalence. *Nat. Rev. Genet.* **9**, 789–796 (2008).
- Stern-Ginossar, N. *et al.* Human microRNAs regulate stress-induced immune responses mediated by the receptor NKG2D. *Nat. Immunol.* **9**, 1065–1073 (2008).
- Jonjić, S., Babić, M., Polić, B. & Krmpotić, A. Immune evasion of natural killer cells by viruses. *Curr. Opin. Immunol.* **20**, 30–38 (2008).
- Powers, C., DeFilippis, V., Malouli, D. & Fruh, K. Cytomegalovirus immune evasion. *Curr. Top. Microbiol. Immunol.* **325**, 333–359 (2008).
- Boss, I.W., Plaisance, K.B. & Renne, R. Role of virus-encoded microRNAs in herpesvirus biology. *Trends Microbiol.* **17**, 544–553 (2009).
- Friedman, R.C., Farh, K.K., Burge, C.B. & Bartel, D.P. Most mammalian mRNAs are conserved targets of microRNAs. *Genome Res.* **19**, 92–105 (2009).
- Choy, M.K. & Phipps, M.E. MICA polymorphism: biology and importance in immunity and disease. *Trends Mol. Med.* **16**, 97–106 (2010).
- Stern-Ginossar, N. & Mandelboim, O. An integrated view of the regulation of NKG2D ligands. *Immunology* **128**, 1–6 (2009).
- Ebert, M.S., Neilson, J.R. & Sharp, P.A. MicroRNA sponges: competitive inhibitors of small RNAs in mammalian cells. *Nat. Methods* **4**, 721–726 (2007).
- Grimson, A. *et al.* MicroRNA targeting specificity in mammals: determinants beyond seed pairing. *Mol. Cell* **27**, 91–105 (2007).
- Saetrom, P. *et al.* Distance constraints between microRNA target sites dictate efficacy and cooperativity. *Nucleic Acids Res.* **35**, 2333–2342 (2007).
- Grey, F. *et al.* Identification and characterization of human cytomegalovirus-encoded microRNAs. *J. Virol.* **79**, 12095–12099 (2005).
- Eissmann, P. *et al.* Multiple mechanisms downstream of TLR-4 stimulation allow expression of NKG2D ligands to facilitate macrophage/NK cell crosstalk. *J. Immunol.* **184**, 6901–6909 (2010).
- Yadav, D., Ngolab, J., Lim, R.S., Krishnamurthy, S. & Bui, J.D. Cutting edge: down-regulation of MHC class I-related chain A on tumor cells by IFN- γ -induced microRNA. *J. Immunol.* **182**, 39–43 (2009).
- Gottwein, E. *et al.* A viral microRNA functions as an orthologue of cellular miR-155. *Nature* **450**, 1096–1099 (2007).
- Skalsky, R.L. *et al.* Kaposi's sarcoma-associated herpesvirus encodes an ortholog of miR-155. *J. Virol.* **81**, 12836–12845 (2007).
- Lu, F. *et al.* Epstein-Barr virus-induced miR-155 attenuates NF- κ B signaling and stabilizes latent virus persistence. *J. Virol.* **82**, 10436–10443 (2008).
- Grey, F., Meyers, H., White, E.A., Spector, D.H. & Nelson, J. A human cytomegalovirus-encoded microRNA regulates expression of multiple viral genes involved in replication. *PLoS Pathog.* **3**, e163 (2007).
- Stern-Ginossar, N. *et al.* Analysis of human cytomegalovirus-encoded microRNA activity during infection. *J. Virol.* **83**, 10684–10693 (2009).

ONLINE METHODS

Lentiviral constructs and transduction. Specific oligonucleotides were annealed and inserted into the pTendoplasmic reticulum vector and then were excised from the vector together with the H1 RNA polymerase III promoter into the lentiviral vector SIN18-pRLL-hEF1p-EGFP-WRPE as described¹⁵. In all experiments, KSHV miR-K12-2 was used as the control microRNA. Specific anti-microRNA sponge oligonucleotides were annealed and inserted into the pBSII phagemid (Stratagene) in two fragments by digestion with the restriction enzymes Sall, HindIII and EcoRI. The full sponge was excised with Sall and EcoRI and was ligated into the lentiviral vector SIN18-pRLL-hEF1p-EGFP-WRPE. In all experiments, the control sponge was a sponge directed against the BART-16 microRNA of EBV. Lentiviruses were produced by transient three-plasmid transfection as described¹⁵. These viruses were used to transduce all the cell lines used and HHF cells in the presence of polybrene (5 g/ml).

RNA and real-time quantitative PCR. For quantitative RT-PCR analysis of mRNA, cDNA was produced from various cells. Total RNA was isolated with TRI reagent (Sigma). RNA was reverse-transcribed with Moloney murine leukemia virus reverse transcriptase (Invitrogen) and random primers (Roche). DNA was amplified with specific primers and Platinum SYBR Green qPCR SuperMix-UDG with ROX (Invitrogen) on an ABI PRISM 7900 real-time PCR system (Applied Biosystems). Total RNA for quantitative RT-PCR analysis of mature microRNA was isolated with TRI reagent (Sigma) and a human total RNA survey panel from Ambion (AM6000) was used. All specimens were polyadenylated with poly(A) polymerase (Ambion). RNA was then reverse-transcribed with Moloney murine leukemia virus reverse transcriptase (Invitrogen) and 0.5 g poly(T) adaptor. Reaction primers were a 3' adaptor primer and primers based on the microRNA sequences.

Cells and viral infection. The RKO, DU145, HeLa, 1190 mel, 1259 mel and Midet cell lines were used. Human fibroblasts were obtained from primary

cultures of foreskins in accordance with the institutional guidelines and permissions for using human tissues. Infection with the TB40 strain of HCMV was done at a multiplicity of infection of 1. Primary NK cells were isolated from healthy donors and were grown as described²⁹.

Flow cytometry and antibodies. Monoclonal anti-MICB (236511) and anti-NKG2D (149810) were from R&D Systems; monoclonal anti-CD99 (12E7; a gift from A. Bernard) served as an isotype-matched control antibody. For flow cytometry, the final concentration of the monoclonal antibody was 0.2 µg per well; the secondary antibody was indodicarbocyanine-conjugated affinity-purified F(ab')₂ fragment of goat anti-mouse IgG (115-175-062, Jackson ImmunoResearch Laboratories). In blocking experiments, the final concentration of the blocking monoclonal antibody to NKG2D was 0.5 µg per well.

Cytotoxicity assay. The *in vitro* cytotoxic activity of NK cells against various target cells was assessed in 5-hour ³⁵S-release assays as described⁴⁷. In all experiments in which blocking antibodies were used, the final concentration was 0.5 µg per well.

Luciferase assay. Construct generation is described in the **Supplementary Methods**. Cells in 24-well plates were transfected using LT1 transfection reagent (Mirus) with 200 ng firefly luciferase reporter vector and 50 ng renilla luciferase pRL-CMV (control; Promega) in a final volume of 0.5 ml. Firefly and renilla luciferase activities were measured consecutively with the Dual-Luciferase Assay system (Promega) 48 h after transfection. Firefly luciferase activity was normalized to renilla luciferase activity and then to the average activity of the control reporter.

47. Mandelboim, O. *et al.* Protection from lysis by natural killer cells of group 1 and 2 specificity is mediated by residue 80 in human histocompatibility leukocyte antigen C alleles and also occurs with empty major histocompatibility complex molecules. *J. Exp. Med.* **184**, 913–922 (1996).